JOURNAL OF GEOPHYSICAL RESEARCH, VOL. 103, NO. A9, PAGES 20,515–20,523, SEPTEMBER 1, 1998

ULF pulsations driven by a randomly varying magnetopause displacement

J. M. Smith, A. N. Wright, and G. J. Rickard[1]
Mathematical Institute, University of St. Andrews, Fife, Scotland

Abstract. A magnetospheric cavity with a two-dimensional profile in Alfvén speed has been driven with a nonmonochromatic source. Detailed numerical results show that the magnetospheric cavity filters the random driving signal and excites preferentially the fast modes whose eigenfrequencies lie within the driving spectrum. These fast modes may also couple to the Alfvén mode, provided $k_y \neq 0$ and their eigenfrequencies lie within the Alfvén continuum. The resulting Alfvén modes and the position of the resonant field lines can be predicted to high accuracy by calculating the natural fast and Alfvén frequencies of the undriven system. A preliminary investigation into the seismology of the magnetosphere has also been undertaken. The ratio of the energy density in the two resonant field lines depends only on the equilibrium of the cavity and not on the nature of the driving source (e.g., initial condition, impulsive excitation, or random forcing). Good agreement is found with the ratio predicted by an approximate analytical treatment based upon the eigenfunctions of the equilibrium magnetosphere. The new seismological technique may prove to be a useful diagnostic tool in future studies.

1. Introduction

The coupling of fast and Alfvén waves has received considerable attention from magnetospheric researchers [e.g., *Southwood*, 1974; *Chen and Hasegawa*, 1974; *Allan et al.*, 1986]. The Alfvén frequency $\omega_A(\mathbf{r})$ is the natural frequency of an Alfvén wave on a field line. For a cavity that is inhomogeneous, $\omega_A(\mathbf{r})$ is constant along a field line, but it varies with position throughout the cavity. The fast mode extends throughout the entire cavity and, unlike the Alfvén mode, is not confined to an individual field line. The coupling between the fast and Alfvén modes depends upon the "azimuthal" wavenumber k_y, with no coupling arising when $k_y = 0$.

Over the last decade, studies have considered wave coupling in two-dimensional (2-D) equilibria analytically in terms of normal modes [*Southwood and Kivelson*, 1986; *Thompson and Wright*, 1993; *Wright and Thompson*, 1994]. Progress has also been made on 2D time-dependent wave coupling [*Lee and Lysak*, 1991; *Wright*, 1992a, b], and these studies indicate that a single fast mode may establish several Alfvén resonances; one on each field line where a natural Alfven frequency matches the fast frequency. The numerical model employed in the present paper is also two-dimensional and demonstrates how one fast mode can drive two Alfvén resonances. We also show how the relative amplitudes of the resonances may be used to study the structure of the equilibrium magnetosphere seismically through its normal modes.

Most previous time-dependent studies have employed initial conditions (which are similar to an impulse) or monochromatic forcing. In this paper we use a novel random magnetopause displacement driving condition. A random driver may be more realistic than the monochromatic drivers considered by some previous studies, since the buffeting of the magnetospheric cavity by the turbulent magnetosheath is unlikely to result in a monochromatic driving source.

Wright and Rickard [1995] give two criteria for driving an Alfvén resonance through a boundary random motion. They considered a cavity with an Alfvén speed inhomogeneity in one direction with linear disturbances under the cold plasma approximation. The driver was found to excite the fast eigenmodes which lie within the frequency spectrum of the driver. Therefore, for a fast mode to be excited its frequency must lie within this spectrum. Second, for the fast mode to drive an Alfvén resonance the fast mode eigenfrequency must lie within the Alfvén continuum. The principal result from *Wright and Rickard* [1995] illustrated that Alfvén waves can be resonantly excited even when the cavity is driven by a nonmonochromatic source. In this chapter we extend

[1]Now at Meteorological Office, Bracknell, England.

Paper number 98JA01460.
0148-0227/98/98JA-01460$09.00

their work by examining randomly driven fast waves in a 2-D inhomogeneous cavity.

Observations of the magnetopause [*Chen et al.*, 1993; *Chen and Kivelson,* 1993, and references therein] show how the magnetopause is often disturbed and can support nonsinusoidal fluctuations with an amplitude of about 0.5 R_E and typical period of 5 min. There is substantial circumstancial evidence that such boundary motions can drive field line resonances with similar periods (i.e., Pc 5 pulsations) through the intermediary of the fast mode. However, direct observations of such fast modes have remained elusive. *Allan et al.* [1997] suggest that the search for a clear monochromatic fast mode signature like that seen in modeling will be unsuccessful, and at best one may see the suggestion of a narrowband driver over a small range of L shells in satellite data. *Rickard and Wright* [1995] treated the magnetosphere as an open-ended cavity (or waveguide) and found that the dispersive nature of the fast mode would obscure any clear monochromatic signature. For these reasons is seems the best signature of magnetospheric fast modes is the indirect evidence of field line resonances.

The format of this paper is as follows. We begin by describing our model and governing equations. Then we give an outline of the numerical scheme for solving the ideal MHD equations and also the algorithm for obtaining a random driving source. Our results are then described. First, we calculate the fast mode eigenfrequencies of the cavity and also the upper and lower frequencies of the Alfvén continuum. The temporal form of the random driver and its Fourier transform is then illustrated. The response of the cavity to the random driver is then discussed, and the coupling between the fast and Alfvén modes is also examined. Applications of this work to the seismological study of the magnetosphere is given, and finally our work is summarized.

2. Governing Equations and Equilibrium

The aim of this paper is to study ULF waves in the Earth's magnetosphere. To undertake this investigation, we begin with the magnetospheric box model [e.g., *Southwood,* 1974]. The cavity is illustrated in Figure 1; its width is L $(0 < x < L)$, and its height is $2L$ $(-L < z < L)$. In this paper we take the magnetic pressure to dominate over the plasma pressure, i.e., the cold plasma approximation. In addition, the magnetic field is assumed to be straight and uniform and is situated between the northern and southern ionospheres (located at $z = \pm L$). The x and y axes represent the radial and azimuthal directions, respectively. The inhomogeneity in Alfvén speed (and density) is taken to vary in both the x and z directions and so is a generalisation of *Southwood*'s [1974] model, which was governed by an ordinary differential equation (ODE). The more general density variation employed here results in a partial differential equation (PDE) problem. The magnetopause

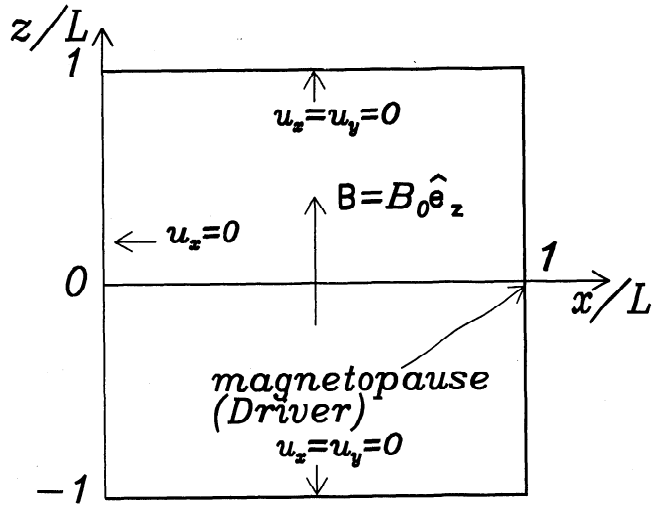

Figure 1. Sketch of the MHD cavity used in our simulations. A uniform magnetic field $\mathbf{B} = B_0\hat{\mathbf{e}}_z$ permeates the cavity. The driver is situated along the $x = L$ field line. On the three boundaries $z = \pm L$ and $x/L = 0$ we employ perfectly reflecting boundary conditions for the fast mode ($u_x = 0$). We take u_y equal to zero at $z = \pm L$.

is taken to lie along the $x = L$ field line. The governing MHD PDEs are solved by a numerical scheme originally developed by *Wright and Rickard* [1995].

The ideal MHD equations governing the (linear) small-amplitude velocity ($\mathbf{u} = (u_x, u_y, 0)$) and magnetic field ($\mathbf{b} = (b_x, b_y, b_z)$) perturbations in the low-β approximation are given by

$$\frac{\partial u_x}{\partial t} = \frac{v_A^2}{B_0}\left(\frac{\partial b_x}{\partial z} - \frac{\partial b_z}{\partial x}\right), \quad (1)$$

$$\frac{\partial u_y}{\partial t} = \frac{v_A^2}{B_0}\left(\frac{\partial b_y}{\partial z} - \frac{\partial b_z}{\partial y}\right), \quad (2)$$

$$\frac{\partial b_x}{\partial t} = B_0\frac{\partial u_x}{\partial z}, \quad (3)$$

$$\frac{\partial b_y}{\partial t} = B_0\frac{\partial u_y}{\partial z}, \quad (4)$$

$$\frac{\partial b_z}{\partial t} = -B_0\left(\frac{\partial u_x}{\partial x} + \frac{\partial u_y}{\partial y}\right), \quad (5)$$

where the square of the Alfvén speed is given by $v_A^2 = B_0^2/\mu_0\rho$, B_0 is the magnitude of the equilibrium magnetic field, and the plasma density is denoted by ρ. We have taken the magnetic field to be uniform; $\mathbf{B} = B_0\hat{\mathbf{e}}_\mathbf{z}$. Under the cold plasma approximation the fast and Alfvén modes are present and the slow mode is absent. When the wavenumber k_y is small, the fast mode is approximately given by u_x, b_x, and b_z, whereas the Alfvén mode is characterized by u_y and b_y [*Wright,* 1992a]. The Alfvén speed profile $v_A(x,z)$ is assumed to be a separable function: $v_A(x,z)/v_{A0} = X(x)\,Z(z)$. Specifically, we use

$$X(x) = 1 - \frac{x}{1.3L}, \quad (6)$$

$$Z(z) = 3 - 2\cos\left(\frac{\pi z}{L}\right) . \quad (7)$$

Here, v_{A0} is the Alfvén speed at $(x/L = 0, z/L = 0)$, and the cavity width is L. In our work we consider the dimensionless frequency of oscillation, defined to be $\omega L/v_{A0}$. The Alfvén speed functions X and Z are plotted in Figure 2.

3. Eigenmodes and Eigenfrequencies

We now calculate the frequencies associated with both the Alfvén continuum and the fast modes, which are of importance for our numerical work. When k_y is small, but nonzero, the fast eigenfrequencies may be estimated by calculating the eigenfrequencies when k_y is set to zero. *Wright* [1994] shows how the fast eigenfrequency (ω_f) is approximately independent of k_y for small k_y: $\partial\omega_f/\partial k_y|_{k_y=0} = 0$, i.e., $\omega_f(k_y) \approx \omega_f(k_y = 0) + O(k_y^2)$. Therefore, to calculate the eigenfrequencies in our coupled system, we take $k_y \ll 1$ and compute the decoupled frequencies. We impose perfectly reflecting boundary conditions for calculating the decoupled eigenfunctions and eigenfrequencies: $\xi_x = \xi_y = 0$ at $z = \pm L$, and $\xi_x = 0$ at $x = 0, L$.

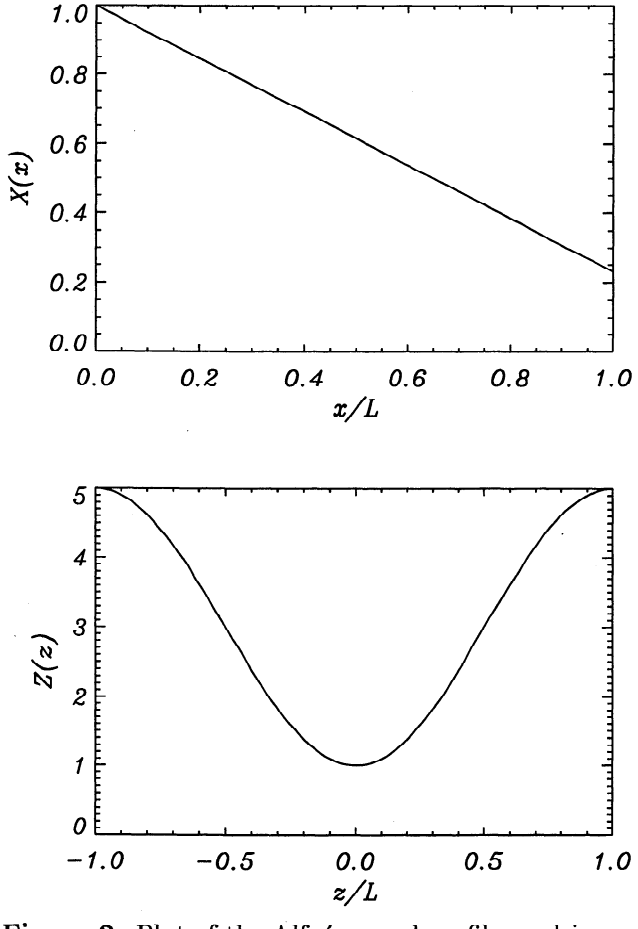

Figure 2. Plot of the Alfvén speed profile used in our study. We take the Alfvén speed $v_A(x,z)$ to be a separable function written as $X(x)Z(z)$. Specifically, we take $X(x) = 1 - (x/1.3L)$ and $Z(z) = 3 - 2\cos(\pi z/L)$.

Table 1. Properties of the Fast Eigenmodes.

Mode	$\omega L/v_{A0}$	Symmetry
1	2.520	S
2	4.216	S
3	4.395	A
4	5.869	S
5	6.014	S
6	6.132	A

The lowest six eigenfrequencies (and the associated eigenfunctions) are calculated by using the eigenvalue code described by *Oliver et al.* [1996; see also *Smith et al.*, 1997]. To obtain these frequencies, we set $k_y = 0$ and use the Alfvén speed profile (equations (6) and (7)) with a uniform magnetic field $\mathbf{B} = B_0\hat{\mathbf{e}}_z$ and a reflecting boundary ($u_x = 0$) at $x/L = 1$. Table 1 gives the dimensionless frequencies and also denotes whether the modes are symmetric (S) or asymmetric (A) about $z/L = 0$. Asymmetric and symmetric modes are characterized by a node and antinode, respectively, in u_x, along $z/L = 0$. Note that only one asymmetric mode exists (mode 3) in the frequency range $0 < \omega L/v_{A0} < 6$.

We now calculate the upper (ω_+) and lower (ω_-) frequencies of the Alfvén continua for the Alfvén speed profile used in our study. Consider the second-order ODE governing the decoupled ($k_y = 0$) Alfvén wave,

$$\frac{d^2\phi}{dz^2} + \frac{\omega_A^2(x)}{v_A^2(x,z)}\phi = 0 . \quad (8)$$

Here, ϕ is the Alfvén wave eigenfunction. When we write the Alfvén speed as $v_A(x,z) = X(x)Z(z)$, equation (8) becomes

$$\frac{d^2\phi}{dz^2} + \frac{\Omega^2}{Z^2}\phi = 0 , \quad (9)$$

where we have defined $\Omega^2(x) = \omega_A^2/X^2$. Equation (9) is solved numerically by applying the boundary conditions $u_y = 0$ at $z = \pm L$. Equation (9) determines the eigenvalues Ω_1^2, Ω_2^2, ... of the Alfvén mode. The frequencies of the Alfvén continuum are then calculated by

$$\omega_{Ai}^2(x) = X^2(x)\,\Omega_i^2 . \quad (10)$$

In addition, to calculate the position of the resonant field lines, we set

$$\omega_f^2 = \omega_{Ai}^2 = X^2(x_{ri})\,\Omega_i^2 , \quad (11)$$

where ω_f is the fast mode eigenfrequency and x_{ri} is the position of the resonant field line.

Table 2 gives the lower and upper frequency limits of the first five Alfvén continua, $\omega_- L/v_{A0}$ and $\omega_+ L/v_{A0}$, respectively. In addition, the fast modes from Table 1 that have frequencies within each continuum range and possess the same symmetry as the Alfvén mode are

Table 2. Alfvén Continua Limits and Resonant Fast Modes.

Harmonic	$\omega_- L/v_{A0}$	$\omega_+ L/v_{A0}$	Fast mode
1	0.5291	2.2928	-
2	1.5834	6.8613	3, 6, ... (A)
3	2.4419	10.5814	1, 2, 4, 5, ... (S)
4	3.2645	14.1462	3, 6, ... (A)
5	4.0765	17.6647	2, 4, 5, ... (S)

given. We also denote whether these modes are symmetric (S) or asymmetric (A).

To proceed further, we shall focus on the asymmetric modes. We notice from Table 2 that the third fast mode (which is asymmetric) will couple to both the second and fourth Alfvén harmonics. From equation (11) we calculate that the second and fourth Alfvén harmonics will have frequencies equal to the third fast mode at locations $x_{r2} = 0.467L$ and $x_{r4} = 0.896L$, when driven by the third fast mode with $\omega_f L/v_{A0} = 4.395$.

4. Time-Dependent Solutions

Previous time-dependent studies of MHD wave coupling in a cavity model have employed a variety of driving conditions. Some have used an impulsive stimulus [*Allan et al.*, 1986; *Lee and Lysak*, 1991], which, following the driving phase, is very similar to an undriven initial condition solution [*Mann et al.*, 1995]. These studies show how a set of fast eigenmodes are excited, which then go on to drive a set of field line resonances in the manner described by *Kivelson and Southwood* [1985]. Other modeling has employed monochromatic driving, which drives solutions that asymptote to normal modes (with frequency equal to that of the driver) if dissipation is present. In one such study, *Steinolfson and Davila* [1993] note that when the cavity is driven at a natural fast eigenfrequency the efficiency with which energy is absorbed from the driven boundary is maximized.

The basis of the numerical code employed in this chapter is described fully by *Wright and Rickard* [1995]. Their one-dimensional code has been modified to investigate ULF wave propagation in a 2-D inhomogeneous cavity. The numerical scheme we employ is *Zalesak*'s [1979] leapfrog-trapezoidal algorithm, which is second-order accurate in both space and time. In our simulations, 480 grid points were used in the x direction, and 240 points were used in the z direction. The time step was chosen to be 0.05 of the minimum propagation time across a cell. Energy conservation was satisfied to within 1 part in 10^6, and the maximum $\nabla \cdot \mathbf{b}$ was 10^{-10}. The velocity and magnetic field perturbations are found by updating $\mathbf{u}$ and $\mathbf{b}$ at every grid point according to the governing equations (1)-(5), except where the driver is located (along $x = L$). Tables 1 and 2 indicate that the third fast mode (which is asymmetric) may drive second and fourth harmonic Alfvén resonances. To focus upon these asymmetric modes, the driving motion at the boundary $x/L = 1$ has an asymmetric variation with z (i.e., a node of u_x at $z = 0$). For $0 < z/L < 0.5$ the displacement of the boundary is described by the envelope function $F(z/L) = \sin(\pi z/L)$. For $z/L > 0.5$ the function is given by $F(z/L) = 0.5(1 - \cos(2\pi z/L))$. Since the driving condition will excite only asymmetric modes of the system, it is necessary to solve only in the region $z > 0$, while applying the symmetry conditions $u_x = u_y = b_z = \partial b_x/\partial z = \partial b_y/\partial z = 0$ at $z = 0$. In addition, along the edges of the cavity $x/L = 0$ and $z/L = \pm 1$, we apply perfectly reflecting boundaries ($u_x = 0$), and u_y is also set to zero at $z = \pm L$.

4.1. Random Driver

The algorithm to obtain the random driving source is described in detail by *Wright and Rickard* [1995]; here we only give a brief outline. A random set of data for the x displacement of the boundary is obtained at discrete times t_n. Two time intervals are specified, Δt_1 and $\Delta t_2 (> \Delta t_1)$. A random number generator gives a value for the boundary displacement between -1 and 1. The time is then determined by $t_n = t_{n-1} + \Delta t$, where the interval Δt is given by either Δt_1 or Δt_2. The probability that Δt_1 is chosen over Δt_2 is taken to be 90%. If Δt_2 is chosen, the next two time steps are given by Δt_1. A cubic spline is then fitted to the discrete points to give a continuous expression for the boundary displacement at all times. The x component of velocity is then obtained by differentiating the continuous function of the boundary displacement. For the simulations undertaken in our work we take $\Delta t_1 = 1$ and $\Delta t_2 = 10$. We measure times in terms of the Alfvén transit time, $t_A = tv_{A0}/L$.

At $t_A = 0$ we impose that both the boundary displacement and its first and second time derivatives are zero. This condition removes any transient effects when the boundary motion starts and is achieved by creating a symmetrical set of data points about $t_A = 0$.

Figure 3a shows the variation of the random driving velocity $u_x(x = L, z = 0.15L)$ with normalized time $\tau \equiv t_A = tv_{A0}/L$. In Figure 3b we show the Fourier transform of the velocity in Figure 3a. The driver has a broadband frequency spectrum lying in the range $0 < \omega L/v_{A0} < 6$, and there is no preferred driving frequency. The dashed line in Figure 3b denotes the frequency of the only asymmetric mode, $\omega_f L/v_{A0} = 4.395$, which exists within the frequency range of the driver. It is important to note that the driver does not favor this frequency. From Table 2 we expect this fast mode to be important in our simulations, along with the second and fourth Alfvén harmonic resonances.

4.2. Cavity Response

In this section we investigate how the cavity responds to the random driving motion when we set $k_y L = 0.01$.

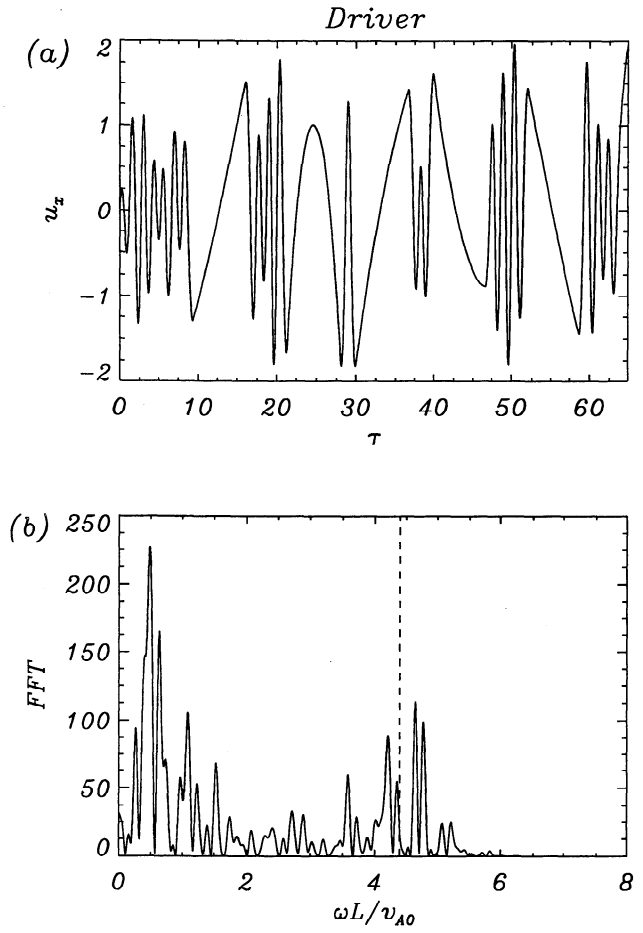

Figure 3. (a) Temporal form of the random driver and (b) Fourier transform of Figure 3a. The velocity u_x is measured at $x = L$, $z = 0.15L$. Notice that the driving source is a broadband spectrum with frequencies lying in the range $0 < \omega L/v_{A0} < 6$. The dashed line denotes the position of the only asymmetric mode that exists within this frequency range. Note that the driver does not favor this frequency.

The reason for choosing a small value of $k_y L$ is that the fast mode frequency will be close to the $k_y = 0$ values given in Table 1. Figure 4a shows the evolution of the x component of the velocity (u_x) at a fixed point ($x/L = 0.93$, $z/L = 0.45$) within the cavity as a function of time. The velocity is much more coherent than the driving motion (compare with Figure 3a), as shown in the Fourier transform of u_x (Figure 4b). The presence of a preferred frequency of oscillation within the cavity is now evident. It is interesting to note that this frequency agrees well with the ($k_y = 0$) third fast mode eigenfrequency calculated from the eigenvalue code [*Oliver et al.*, 1996]. Notice that the sixth fast mode frequency, $\omega_f L/v_{A0} = 6.132$, is not excited, since it lies outside the frequency range of the driver (see Figure 3b).

Since k_y is small, Figure 4a essentially gives the temporal variation of the fast mode at a fixed location within the cavity. It is evident that the cavity filters the random driving source and frequencies that are not eigenfrequencies of the cavity are suppressed. The cavity oscillates in a quasi-monochromatic fashion, since it is dominated by power in a very narrow frequency range.

The fast eigenmodes in the cavity are excited provided their eigenfrequencies lie within the spectrum of the driver and they share the same field-aligned symmetry as the driver. This finding is in agreement with the results of *Wright and Rickard* [1995]. This result may be understood by considering physical analogies, for example, blowing air across an empty bottle or playing a wind instrument. Even though the source of the sound is broadband, the instrument or bottle enhances characteristic frequencies.

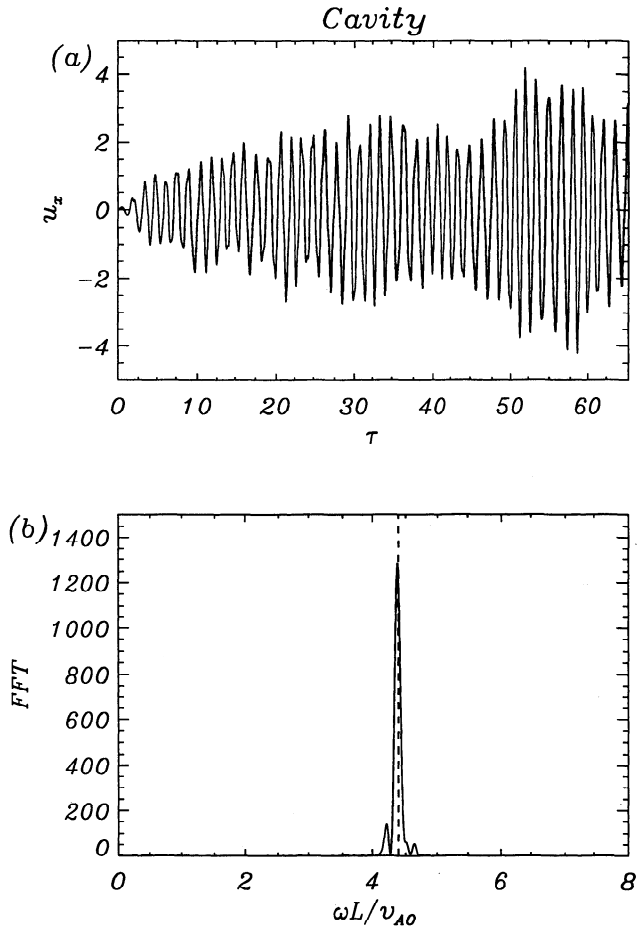

Figure 4. (a) The x-component of velocity (characteristic of the fast mode) at the location ($x/L = 0.93$, $z/L = 0.45$) in the cavity. Notice that the oscillation is more coherent than the driving motion (Figure 3a). (b) Fourier transform of Figure 4a. The dashed line shows the frequency of the first asymmetric mode at a dimensionless frequency of $\omega_f L/v_{A0} = 4.395$. The frequency of the fast mode within the cavity is equal to $\omega_f L/v_{A0}$. The cavity therefore acts as a filter, suppressing frequencies that are not eigenfrequencies of the system, allowing cavity eigenmodes to dominate the solution.

To summarize, we have driven a cavity with a broadband spectrum $0 < \omega L/v_{A0} < 6$. Within this frequency range we have calculated that one asymmetric frequency exists ($\omega_f L/v_{A0} = 4.395$). The cavity extracts this eigenfrequency from the driver, suppressing all other frequencies. Having seen that a nonmonochromatic driver is able to excite a quasi-monochromatic fast mode, we now examine how this mode may couple to an Alfvén wave.

4.3. Fast and Alfvén Mode Coupling

If $k_y = 0$ the fast and Alfvén modes are decoupled, whereas if $k_y \neq 0$ there is coupling between the two modes. The condition for the fast magnetoacoustic mode to drive an Alfvén resonance is that the frequency must lie within the Alfvén continuum. From the Alfvén speed profile we employ, two resonant field lines are expected to exist within the cavity. These correspond to the fast mode eigenfrequency $\omega_f L/v_{A0} = 4.395$, occurring at locations $x_{r2} = 0.467L$ and $x_{r4} = 0.896L$. Here the subscripts 2 and 4 refer to the second and fourth harmonics of the Alfvén mode, respectively. The sixth fast mode, with a frequency of $\omega_f L/v_{A0} = 6.132$, is not excited, since it lies outside the driving spectrum (see Figure 4b). Therefore we do not expect this fast mode to drive any Alfvén resonances.

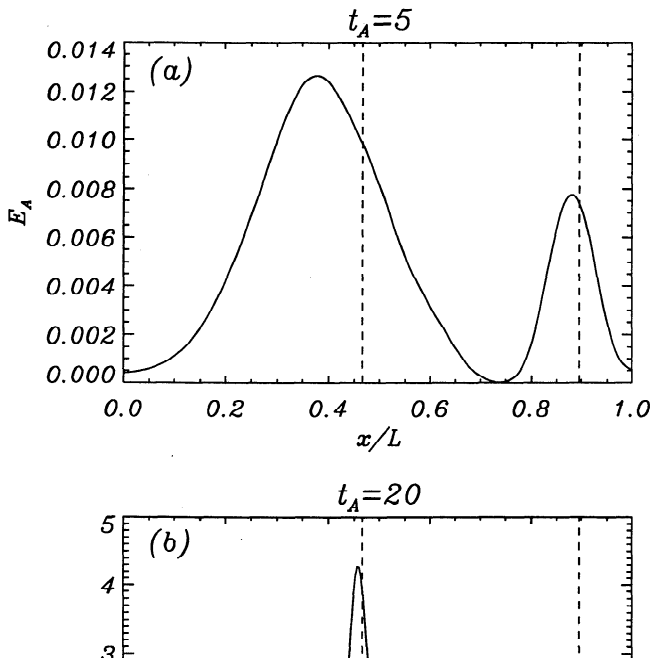

Figure 5. The Alfvén energy E_A $(= \frac{1}{2}\rho u_y^2 + b_y^2/2\mu_0)$ at $z/L = 0.05$ at times (a) $t_A = 5$ and (b) $t_A = 20$, using $k_y = 0.01$. The period of the waves is $1.43a/v_{A0}$. The dashed lines denote the locations of the calculated resonances assuming a monochromatic driver. Notice that as time increases, the Alfvén wave energy becomes more localized about the resonant field lines. These are located at $x_{r2} = 0.467L$ and $x_{r4} = 0.896L$, corresponding to the second and fourth harmonics of the Alfvén mode, respectively.

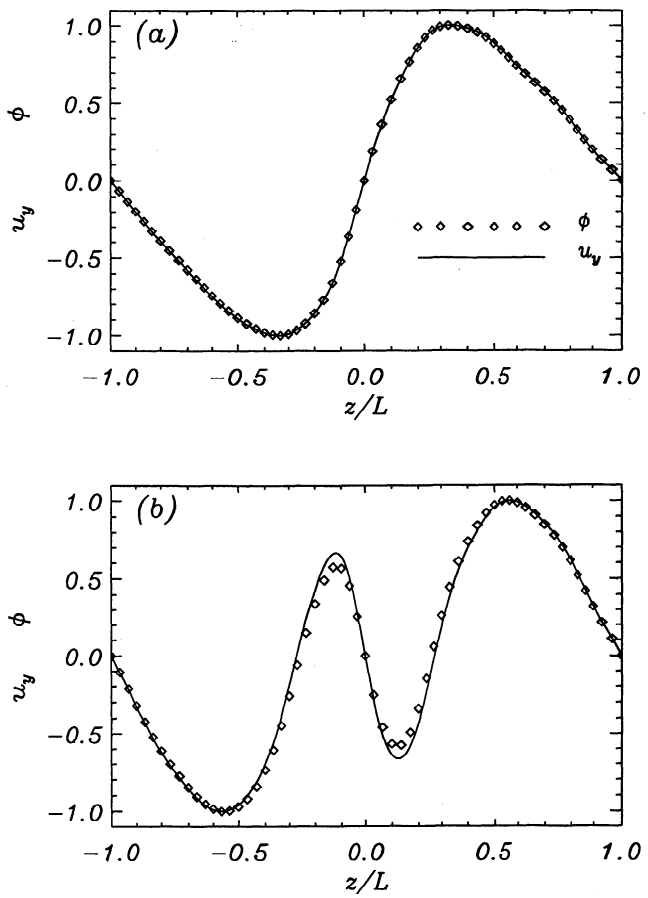

Figure 6. The (a) second and (b) fourth harmonics of the Alfvén wave eigenfunction ϕ. The solid line denotes u_y along each resonant field line, calculated from the time-dependent code, measured after 20.0 Alfvén times. The eigenfunction calculated by solving the ordinary differential equation (equation (8)) is shown by diamond symbols. The agreement between the two cases is excellent.

In Figure 5 we plot the Alfvén wave energy E_A $(= \frac{1}{2}\rho u_y^2 + b_y^2/2\mu_0)$ as a function of x/L for $z/L = 0.05$ at two times. Figures 5a and 5b illustrate E_A at times $t_A = 5$ and $t_A = 20$, respectively. The dashed lines denote the positions of the two predicted resonant field lines at x_{r2} and x_{r4} (assuming a fast mode frequency of $\omega_f L/v_{A0} = 4.395$). At early times (Figure 5a) the Alfvén energy density is broad, although it is primarily located around the resonant field lines. As time increases, the resonances becomes much sharper and occur along the predicted field lines (Figure 5b). (The width of the resonances is expected to be proportional

to $1/t_A$ [*Mann et al.*, 1995].) It appears that the random driving motion can excite a fast eigenmode, which can then drive an Alfvén resonance in much the same way as a monochromatic driver.

This result can be confirmed by examining the Alfvén mode eigenfunctions. In Figures 6a and 6b we show u_y calculated from our time-dependent simulations (solid line) for the field lines at x_{r2} and x_{r4}, respectively, measured after 20.0 Alfvén times. In addition, we have overplotted the Alfvén continuum eigenfunction ϕ calculated by solving the ordinary differential equation (9) along each resonant field line with a Runge Kutta scheme. The agreement between the time-dependent calculation with the random driver and the continuum eigenmode confirms the excitation of two Alfvén resonances even if a random driver is used.

4.4. Relation to Observations

It is worth comparing the frequencies observed in data with those generated in our model. The lowest-frequency Pc 5 waves on the flanks have a frequency of the order of 1 mHz. The lowest eigenfrequency of our system is (see Table 1) 2.52 v_{A0}/L. To get a dimensional frequency from this, we need to specify values for the radial extent of the cavity and the Alfvén speed. By assuming $L = 15\ R_E$ we can turn this calculation around by asking what the implied Alfvén speed is in the equatorial plane just inside the magnetopause if our eigenfrequency of 2.52 corresponds to 1 mHz. The implied Alfvén speed (calculated with the aid of Figure 2) is about 60 km/s, which is a little low. However, this underestimate is in keeping with other models which have had to enhance the magnetospheric density (i.e., depress the Alfvén speed) in order to get agreement with observations.

How the magnetosphere generates such low-frequency oscillations is still an outstanding problem, and an important one. It may be that our simple uniform field model, which neglects the curved geometry of the magnetospheric field and its variation with radius, is too crude. Alternatively, it may be that the boundary conditions we are applying at the magnetopause and inner magnetosphere are not appropriate.

The absence of clear cavity mode signatures in data has caused some concern recently. As we mentioned in section 1, this can probably be explained quite naturally in terms of the waveguide nature of the magnetospheric flanks or the finite lifetime of drivers in a dissipative or leaky cavity.

5. Seismology of the Magnetosphere

We now give details about how the work described in this chapter may extend the seismological study of the magnetosphere. For each Alfvén resonance we calculated the Alfvén wave energy per unit area perpendicular to the resonant field line

$$E_{di} = \int_{x=x_{ri}} E_A dz \tag{12}$$

E_d is proportional to the amplitude squared of the Alfvén wave and is convenient to work with as it does not oscillate in time. In Figure 7 we plot the ratio E_{d2}/E_{d4} as a function of time for the random driver (Figure 7a), a monochromatic driver (Figure 7b), and an initial condition (Figure 7c). In Figure 7b the monochromatic driver has a frequency equal to the fast eigenfrequency (4.395) and was ramped up over half a cycle so that $u_x = \partial u_x/\partial t = 0$ at $t_A = 0$. In Figure 7c we read the initial u_x from the eigenvalue/eigenfunction code [*Oliver et al.*, 1996] employed in the $k_y = 0$ mode calculations described earlier. The boundary $x = L$ is held as a reflecting boundary ($u_x = 0$) in Figure 7c. In all parts of Figure 7 we use $k_y L = 0.1$. The three cases show that the energy ratio is independent of the driving source. The initial transient stage does exhibit differences, but after only four cycles ($t_A = 6$) all three cases show the energy ratio to be approximately equal to 3.5.

For the case shown in Figure 7 we may use analytical results obtained by *Wright* [1992a] to find that the ratio of Alfvén energy densities E_d (integrated along the field lines) for the two resonant field lines tends to a constant value for increasing time. The energy ratio of the two resonant field lines is given by

$$\frac{E_{d2}}{E_{d4}} = \frac{X^2(x_{r2})}{X^2(x_{r4})}\left[\frac{\int_{x_{r2}} \phi_r(x_{r2})(\partial\xi_x/\partial x)\mathrm{d}z}{\int_{x_{r4}} \phi_r(x_{r4})(\partial\xi_x/\partial x)\mathrm{d}z}\right]^2 \times \frac{\int_{x_{r4}} (\phi_r(x_{r4})/Z)^2\,\mathrm{d}z}{\int_{x_{r2}} (\phi_r(x_{r2})/Z)^2\,\mathrm{d}z}, \tag{13}$$

where the subscripts 2 and 4 denote the second and fourth harmonics, respectively. In addition, X and Z are the separable functions that determine the Alfvén speed profile, given by equations (6) and (7). The function ϕ_r is the Alfvén wave eigenfunction (defined in (9)), and ξ_x is the fast mode displacement.

Inserting the appropriate quantities into this equation, we obtain a ratio that is too large by a factor of 2. It is encouraging that the numerically and analytically derived energy ratios are in rough agreement, although it is desirable to improve the analytical result.

That the energy ratio is independent of the nature of the driver is perhaps surprising but may be understood as follows: The three types of driver (random, monochromatic at the fast eigenfrequency, and an initial condition corresponding to the fast eigenmode) all establish a fast mode in the cavity whose structure is predominantly that of the fast eigenmode. This was confirmed by producing contour plots of b_z and u_x for the three drivers in the large time limit and comparing them with the corresponding decoupled eigenmode plots ($k_y = 0$). Once it is realized that each driver excites the same fast mode structure, it is then natural for

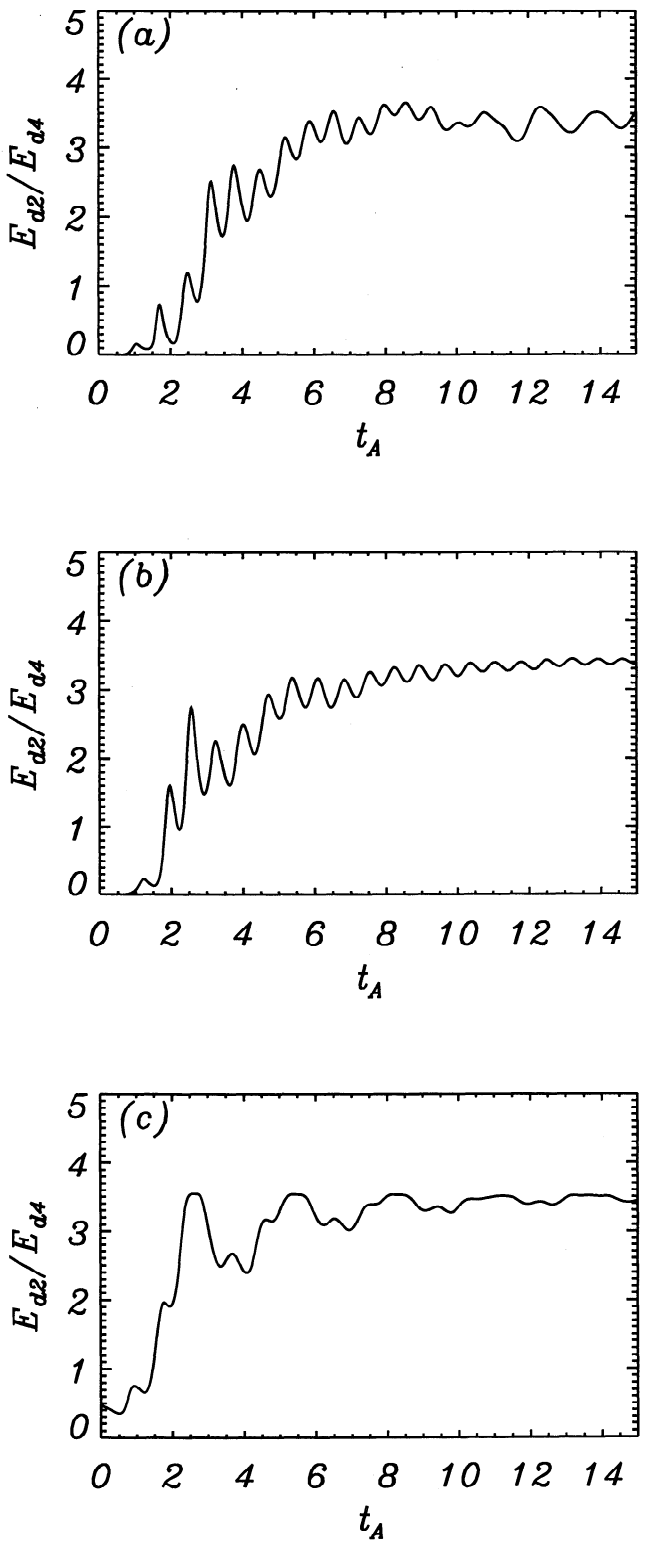

Figure 7. The energy ratio of the the Alfvén mode E_{d2}/E_{d4} in the two resonant field lines at x_{r2} and x_{r4}. The ratio of the energy of the second harmonic to the fourth harmonic is plotted as a function normalized time with $k_y = 0.1$ using (a) a random driver, (b) a monochromatic driver (constant frequency), and (c) u_x obtained from the eigenvalue code (section 3) as the initial condition. In all three cases the energy ratio approaches the same constant value. The energy ratio is therefore independent of the nature of the driving source and depends only on the equilibrium of the cavity.

each driver to excite Alfvén resonances with the same relative amplitudes and energy densities.

The fast mode established by all the drivers is predominantly the decoupled fast eigenmode and thus is determined solely by the equilibrium of the magnetosphere and appropriate boundary conditions. Note that although the amplitude of any given eigenmode will depend upon the form of the driving function along the magnetopause boundary, the structure of the eigenmode was found to be very insensitive to it, particularly when the mode had achieved a significant amplitude and the magnetopause became an approximate node of the eigenmode. Consequently, all the functions and positions in (12) are determined by the equilibrium magnetosphere. Hence changing the equilibrium model will modify the energy ratio, and this quantity may be used as a diagnostic of the equilibrium field and density distributions.

It is worth noting that if dissipative ionospheric boundary conditions are introduced the energy ratio of the two resonances will change. The resonances are still excited by the fast mode supplying a given (different) time-averaged energy flux to each resonance. The dissipative resonances will not grow secularly but will saturate at an amplitude where the time-averaged ionospheric energy dissipation balances the fast energy supply. The energy ratio now depends upon the height-integrated Pederson conductivity at the foot of each field line, in addition to the equilibrium magnetosphere structure.

6. Summary

In this paper we have investigated the effects of a random driver on an MHD cavity. We have shown that a broadband driver excites the fast magnetoacoustic modes whose eigenfrequencies lie within the frequency range of the driver. The fast modes may couple to an Alfvén mode, provided the fast mode frequency lies within the Alfvén continuum and the wavenumber k_y is nonzero. The position and eigenfunction of the Alfvén resonance may be accurately calculated by taking the driving frequency to be monochromatic.

A preliminary investigation into the seismology of the magnetosphere has also been undertaken. The ratio of the field line Alfvén wave energy density of the two resonant field lines tends to a constant value. This value is independent of the driving mechanism and depends only on the equilibrium of the cavity.

Acknowledgments. J.M.S. is supported through a EPSRC studentship and is grateful to Ramon Oliver for use of the eigenvalue code. A.N.W. is supported via a PPARC Advanced Fellowship. G.J.R. was supported by PPARC.

The Editor thanks Dong-Hun Lee and another referee for their assistance in evaluating this paper.

References

Allan, W., S. P. White, and E. M. Poulter, Impulse-excited hydromagnetic cavity and field-line resonances in the magnetosphere, *Planet. Space Sci., 34*, 371, 1986.

Allan, W., A. N. Wright, and D. R. McDiarmid, Spacecraft transits across simulated field line resonance regions, *J. Geophys. Res, 102*, 14,407, 1997.

Chen, L., and A. Hasegawa, A theory of long-period magnetic pulsations, 2, Impulse excitation of surface eigenmode *J. Geophys. Res., 79*, 1033, 1974.

Chen, S.-H., and M. G. Kivelson, On nonsinusoidal waves at the Earth's magnetopause, *Geophys. Res. Lett., 20*, 2699, 1993.

Chen, S.-H., M. G. Kivelson, J. T. Gosling, R. J. Walker, and A. J. Lazarus, Anomalous aspects of magnetosheath flow and of the shape and oscillations of the magnetopause during an interval of strongly northward interplanetary magnetic field, *J. Geophys. Res., 98*, 5727, 1993.

Kivelson, M. G., and D. J. Southwood, Resonant ULF waves: A new interpretation, *Geophys. Res. Lett., 12*, 49, 1985.

Lee, D. H., and R. L. Lysak, Impulsive excitation of ULF waves in the three-dimensional dipole model: The initial results, *J. Geophys. Res., 96*, 3479, 1991.

Mann, I. R., A. N. Wright, and P. S. Cally, Coupling of magnetospheric cavity modes to field line resonances: A study of resonance widths, *J. Geophys. Res., 100*, 19,441, 1995.

Oliver, R., A. W. Hood, and E. R. Priest, MHD waves in solar coronal arcades, *Astrophys. J., 461*, 424, 1996.

Rickard, G. J., and A. N. Wright, ULF pulsations in a magnetospheric waveguide: Comparison of real and simulated satellite data, *J. Geophys. Res., 100*, 3531, 1995.

Smith, J. M., B. Roberts, and R. Oliver, Ducted waves in coronal loops: Curvature effects, *Astron. and Astrophys., 317*, 752, 1997.

Southwood, D. J., Some features of field line resonances in the magnetosphere, *Planet. Space Sci., 22*, 483–491, 1974.

Southwood., D. J., and M. G. Kivelson, The effect of parallel inhomogeneity on magnetospheric hydromagnetic wave coupling, *J. Geophys. Res., 91*, 6871, 1986.

Steinolfson, R. S., and J. M. Davila, Coronal heating by the resonant absorption of Alfvén waves: Importance of the global mode and scaling laws, *Astrophys. J., 415*, 354, 1993.

Thompson, M. J., and A. N. Wright, Resonant Alfvén wave excitation in two-dimensional systems: Singularities in partial differential equations, *J. Geophys. Res., 98*, 15,551, 1993.

Wright, A. N., Coupling of fast and Alfvén modes in realistic magnetospheric geometries, *J. Geophys. Res., 97*, 6429, 1992a.

Wright, A. N., Asymptotic and time-dependent solutions of magnetic pulsations in realistic magnetic field geometries, *J. Geophys. Res., 97*, 6439, 1992b.

Wright, A. N., Dispersion and wave coupling in inhomogeneous MHD waveguides, *J. Geophys. Res., 99*, 159, 1994.

Wright, A. N., and G. J. Rickard, A numerical study of resonant absorption in a magnetohydrodynamic cavity driven by a broadband spectrum, *Astrophys. J., 444*, 458, 1995.

Wright, A. N., and M. J. Thompson, Analytical treatment of Alfvén resonances and singularities in nonuniform magnetoplasmas, *Phys. Plasmas, 1*, 691, 1994.

Zalesak, S. T, Fully multidimensional FCT algorithms for fluids, *J. Comput. Phys., 31*, 335, 1979.

G. J. Rickard, Meteorological Office, London Road, Bracknell, Bershire, England RG12 2SY. (e-mail: gjrickard@meto.gov.uk)

J. M. Smith and A. N. Wright, Mathematical Institute, University of St. Andrews, Fife KY16 9SS, Scotland. (e-mail: jason@dcs.st-and.ac.uk; andy@dcs.st-and.ac.uk)

(Received January 21, 1998; revised April 2, 1998; accepted April 21, 1998.)